

Rapid communication

Structural change in a series of protonated layered perovskite compounds, $HLnTiO_4$ ($Ln = La, Nd$ and Y)

Shunsuke Nishimoto^a, Motohide Matsuda^a, Stefanus Harjo^b, Akinori Hoshikawa^b, Takashi Kamiyama^b, Toru Ishigaki^c, Michihiro Miyake^{a,*}

^aDepartment of Environmental Chemistry and Materials, Okayama University, Tsushima-Naka, Okayama 700-8530, Japan

^bInstitute for Materials Structure Science, High Energy Accelerator Research Organization, Tsukuba, Ibaraki 305-0801, Japan

^cDepartment of Materials Science and Engineering, Muroran Institute of Technology, Muroran, Hokkaido 050-8585, Japan.

Received 16 November 2005; received in revised form 4 February 2006; accepted 16 March 2006

Available online 22 March 2006

Abstract

A deuterated $n = 1$ Ruddlesden–Popper compound, $DLnTiO_4$ ($HLnTiO_4$, $Ln = La, Nd$ and Y), was prepared by an ion-exchange reaction of Na^+ ions in $NaLnTiO_4$ with D^+ ions, and its structure was analyzed by Rietveld method using powder neutron diffraction data. The structure analyses showed that $DLaTiO_4$ and $DNdTiO_4$ crystallized in the space group $P4/nmm$ with $a = 3.7232(1)$ and $c = 12.3088(1) \text{ \AA}$, and $a = 3.7039(1)$ and $c = 12.0883(1) \text{ \AA}$, respectively. On the other hand, $DYTiO_4$ crystallized in the space group $P2_1/c$ with $a = 11.460(1)$, $b = 5.2920(4)$, $c = 5.3628(5) \text{ \AA}$ and $\beta = 90.441(9)^\circ$. The loaded protons were found to statistically occupy the sites around an apical oxygen of TiO_6 octahedron in the interlayer of these compounds, rather than Na atom sites in $NaLnTiO_4$.

© 2006 Elsevier Inc. All rights reserved.

Keywords: Layered perovskite; Ruddlesden–Popper phase; Ion-exchange; Crystal structure; Neutron diffraction

1. Introduction

Protonated forms of layered perovskite compounds have attracted considerable attention because of the proton conduction and Brønsted acid, which brings intercalation compounds with a variety of organic bases [1–5]. However, circumstances of the protons have not been investigated enough, although the protons loaded in the interlayer induce interesting physical and chemical properties. The crystal structure analysis of deuterated layered perovskite compounds by Rietveld method, using powder neutron diffraction data, brings the precise framework structure including the protons loaded in the interlayer, which could help scientists explain physical and chemical properties of these compounds.

Recently, we have reported the structure refinement of $HLaTiO_4$ ($DLaTiO_4$) [6], which is a layered perovskite compound categorized as a Ruddlesden–Popper family

with the general formula of $A'_2[A_{n-1}B_nO_{3n+1}]$ (A and $A' =$ alkali, alkaline or rare earth, $B =$ transition metal) [7]. The crystal structure of the parent $NaLnTiO_4$ reportedly depends on the size of Ln^{3+} ion [8]. This result predicts that the crystal structure of protonated compound, $HLnTiO_4$ ($Ln =$ rare earth), which was prepared by an ion-exchange reaction from $NaLnTiO_4$ [9], is also dependent on the size of Ln^{3+} ion. The structural analysis by XRD previously reported that $HLnTiO_4$ ($Ln = La, Nd, Sm$ and Gd), however, was isostructural with each other [9]. Then, we have performed the structure refinements of $DLaTiO_4$ ($HLaTiO_4$), $DNdTiO_4$ ($HNdTiO_4$) and $DYTiO_4$ ($HYTiO_4$) by Rietveld method using powder neutron diffraction data in order to clarify the relation between the size of Ln^{3+} ion and crystal structure. In this paper, we present the structure refinements of a series of deuterated Ruddlesden–Popper compounds, $DNdTiO_4$ and $DYTiO_4$, and discuss these compounds along with $DLaTiO_4$ from the point of view of crystal chemistry. Deuterium was used instead of hydrogen in the protonated layered perovskite compounds for neutron diffraction measurement, because hydrogen with

*Corresponding author. Fax: +81 86 251 8906.

E-mail address: mmiyake@cc.okayama-u.ac.jp (M. Miyake).

a large incoherent scattering cross section brings an extreme increase of background, i.e., a decrease of S/N ratio.

2. Experimental

The starting compound, NaLnTiO_4 ($\text{Ln} = \text{Nd}$ and Y), was prepared by the conventional solid-state reaction [8,10–12]. Prior to the preparation, Ln_2O_3 was predehydrated at 900 °C for 9 h, because Ln_2O_3 agent contains a small amount of $\text{Ln}(\text{OH})_3$. Stoichiometric amounts of TiO_2 and Ln_2O_3 and 30% excess of Na_2CO_3 were mixed, and heated at 950 °C for NaNdTiO_4 and at 1000 °C for NaYTiO_4 for 30 min, respectively. The products were washed to remove excess Na_2O with distilled water and dried at 160 °C. Deuterium exchanges of NaNdTiO_4 and NaYTiO_4 were carried out in deuterium chloride, DCl, solutions of 0.1 M (mol dm^{-3}), which were adjusted by deuterium oxide, D_2O , at room temperature in N_2 atmosphere for 12 and 36 h, respectively. The products were washed with D_2O and dried at room temperature in N_2 atmosphere. The products were identified by powder X-ray diffraction (XRD), using a Rigaku RINT2100/PC diffractometer with monochromated $\text{CuK}\alpha$ radiation, and the ion-exchange ratio was determined by measuring pH value and Na^+ ion concentration in filtrate, using a TOA HM-5S pH meter and a Shimadzu AA6800 atomic absorption spectrometer, respectively.

The neutron diffraction data of deuterated specimens were measured on a time-of-flight (TOF) neutron diffractometer at room temperature, using *Vega* at the pulsed spallation neutron facility KENS, High Energy Accelerator Research Organization in Japan. The specimens of ca. 5 g were sealed in a vanadium tube in Ar atmosphere, and set on the diffractometer. The observed data as a function of time were converted into those as a function of d values, referring to intensity data observed in a separate measurement of Si powder as a standard sample. The collected diffraction data were analyzed by Rietveld method, using the program RIETAN-TN for TOF neutron diffraction [13,14].

3. Results and discussion

The XRD patterns and lattice parameters of the parent NaNdTiO_4 and NaYTiO_4 matched with those in a previous report [8]. According to the previous report, the crystal structure of the parent NaLnTiO_4 ($\text{Ln} = \text{rare earth}$) is dependent on the size of Ln^{3+} ions as follows. NaLnTiO_4 ($\text{Ln} = \text{La–Nd}$) compound crystallizes in the tetragonal system with the ideal TiO_6 octahedral connections. On the other hand, NaLnTiO_4 ($\text{Ln} = \text{Sm–Lu}$ and Y) compound crystallizes in the orthorhombic system with the mutual tilting of TiO_6 octahedra. That is, NaNdTiO_4 crystallized in the tetragonal system with the space group $P4/nmm$, while NaYTiO_4 crystallized in the orthorhombic system with the space group $Pbcm$.

The pH values and Na^+ ion concentrations of the DCl solutions increased during the contact with NaNdTiO_4 and NaYTiO_4 . The amounts of uptaken D^+ ions, which were estimated from the pH change, and released Na^+ ions, which were estimated from atomic absorption, agreed with each other for both compounds. Furthermore, the amount of released Na^+ ions attained 100% of Na contents in the samples used. From these results, it was found that all Na^+ ions of NaNdTiO_4 and NaYTiO_4 were perfectly exchanged with D^+ ions. In contrast to the parent compound, NaLnTiO_4 , the structure of the protonated compound, HLnTiO_4 ($\text{Ln} = \text{La, Nd, Sm}$ and Gd), was reported to belong to the tetragonal system with the space group $P4/nmm$ and be independent of the size of Ln^{3+} ions [9]. The XRD peaks corresponding to the basal spacing of DNdTiO_4 and DYTiO_4 shifted toward the higher diffraction angle (2θ) side, compared with the parent NaNdTiO_4 and NaYTiO_4 , respectively. The XRD patterns of both the resulting DNdTiO_4 and DYTiO_4 were indexed as the space group $P4/nmm$, referring to the result of HLnTiO_4 ($\text{Ln} = \text{La, Nd, Sm}$ and Gd) [9]. Therefore, the resulting materials were employed in the measurement for the neutron diffraction.

As the neutron diffraction data of both DNdTiO_4 and DYTiO_4 included diffraction peaks of the vanadium sample holder, the refinements were performed as a mixture of two phases. For the refinements, the constraints were applied to the site occupancy factors for all atoms, assuming that the composition ratios of the samples were ideal values. Furthermore, isotropic temperature factors were applied to all atoms. Starting structural models of DNdTiO_4 were constructed, referring to the result of DLaTiO_4 [6], because the XRD pattern indicated that HNdTiO_4 was isostructural with HLaTiO_4 . The atomic positional data of DLaTiO_4 were used as initial parameters, and the crystal structure of DNdTiO_4 was refined in the space group $P4/nmm$. After several cycles of the least-square refinements, the observed and calculated diffraction patterns were in good agreement with each other as illustrated in Fig. 1.

Although the XRD pattern suggested that the crystal structure of DYTiO_4 belongs to the tetragonal symmetry with the space group $P4/nmm$, some of the observed neutron diffraction peaks were too broad to index on the basis of the tetragonal system. This suggests that some diffraction peaks overlap with one another. Therefore, the refinement of DYTiO_4 was first performed using two structural models; one is a model isostructural with DNdTiO_4 , belonging to the tetragonal symmetry with the space group $P4/nmm$, and the other is a model based on the parent NaYTiO_4 , belonging to the orthorhombic symmetry with the space group $Pbcm$ [8]. In both the models, the D atom was set at the general position in a manner similar to that of DNdTiO_4 structural model, and the constraints were applied to the bond distance and bond angle between Ti and O atoms as well as the site occupancy factors. However, neither of the patterns calculated by

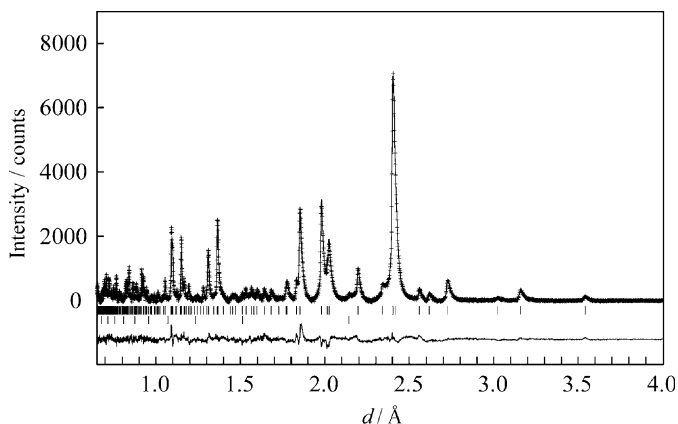


Fig. 1. Observed (plus signs), calculated (solid line) and difference (solid line on the bottom) patterns for TOF neutron powder diffraction of DNdTiO₄. Vertical marks represent positions calculated for Bragg reflections (upper; DNdTiO₄ and lower; Vanadium holder).

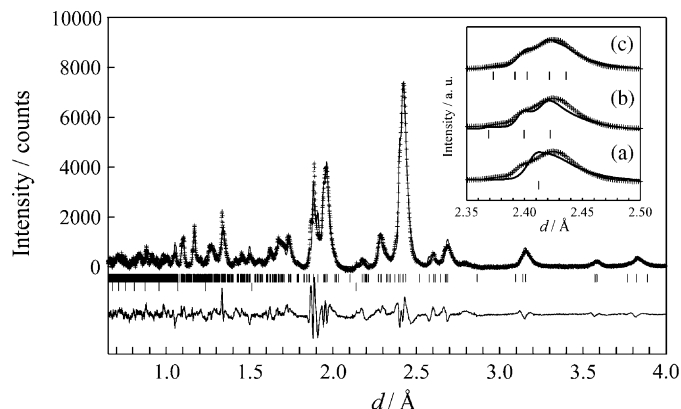


Fig. 2. Observed (plus signs), calculated (solid line) and difference (solid line on the bottom) patterns for TOF neutron powder diffraction of DYTio₄. Vertical marks represent positions calculated for Bragg reflections (upper; DYTio₄ and lower; Vanadium holder). Comparison between selected observed and calculated peak profiles based on the space group (a) *P4/nmm*, (b) *Pbcm* and (c) *P2₁/c*.

these two models gave good fitness to the observed patterns. The comparisons between observed and calculated patterns of the strongest peak at around $d = 2.42 \text{ \AA}$ on the diffraction pattern of DYTio₄ are shown in inset of Fig. 2. The result indicated that the broad peak included extra shoulders at $d \cong 2.44 \text{ \AA}$, which could not be explained by referring to tetragonal cell with the space group *P4/nmm* or orthorhombic cell with the space group *Pbcm*. Moreover, some isotropic temperature factors' values became negative after refining these structural models. Consequently, it was considered that DYTio₄ crystallized in the lower symmetry than the orthorhombic symmetry. Then, the third structural model with the monoclinic cell was constructed. The crystal structure was refined in the space group *P2₁/c*, which is one of the subgroups of the space group *Pbcm*. The orientations of *a*-, *b*- and *c*-axes in the space group *P2₁/c* system correspond to those of *c*-axis and *a*₁- and *a*₂- axes rotated with $-\pi/4$ around *c*-axis in the space group *P4/nmm* system, respectively. The atomic positional data of DYTio₄ based on *Pbcm* were converted into those based on *P2₁/c*, and used as initial parameters. As a result, the fitness between the observed and calculated patterns of the broad peak at $d \cong 2.42 \text{ \AA}$ was significantly improved, as shown in Fig. 2(c), and all the peaks were indexed on the basis of the monoclinic symmetry with the space group *P2₁/c*. However, the refinement revealed that this structural model was still poor, because the isotropic temperature factor of D atom and the standard deviations of isotropic temperature factors of Ti and Y atoms became considerably large. Therefore, the structural model, where the D atom was split into two different sites, i.e., D1 and D2, was adopted in the refinement processes. The site occupancy factor of D1 atom was employed as a parameter and that of D2 atom was reset. As a result, all the atomic parameters converged into reasonable values. The observed and calculated patterns of DYTio₄ obtained after

several cycles of the least-square refinement were illustrated in Fig. 2.

As the refined crystal structure of DYTio₄ by the neutron diffraction study was different from that suggested by the XRD study, re-indexing the XRD data of HYTiO₄ was carried out on the basis of the monoclinic system. As a result, all the observed peaks could be indexed on the basis of the monoclinic system as well as the tetragonal system. This is elucidated as follows; because it is difficult for XRD to observe the reflections arisen from light elements such as protons in compounds containing heavy elements, some reflection peaks could not be detected in the XRD analysis. Consequently, the monoclinic system with the space group *P2₁/c* was adopted as the space group of DYTio₄. The final structural parameters and *R* factors of DNdTiO₄ and DYTio₄, along with DLaTiO₄ are listed in Table 1.

The refined structural illustrations of DNdTiO₄ and DYTio₄ are shown in Fig. 3, together with that of DLaTiO₄. The structure of DLaTiO₄ (*Ln* = La, Nd and Y) consists of (a) TiO₆ octahedral layers, (b) D interlayers and (c) LnO₉ polyhedral layers ordered with a sequence of $-(a)-(b)-(a)-(c)-(a)-$ along the *c*-axis for DLaTiO₄ and DNdTiO₄ and the *a*-axis for DYTio₄. In the DLaTiO₄ and DNdTiO₄ structures, the TiO₆ octahedra with the Ti–O equatorial and mean apical bond lengths of 1.934(1) and 2.25 Å for DLaTiO₄ and 1.918(1) and 2.21 Å for DNdTiO₄, respectively, were ideally connected to each other in a manner similar to those of the parent NaLaTiO₄ and NaNdTiO₄ [8]. On the other hand, the TiO₆ octahedra with the mean Ti–O equatorial and apical bond lengths of 1.975 and 2.12 Å for DYTio₄, respectively, were distorted, and connected to each other with the mutual tilting in a manner similar to those of the parent NaYTio₄ [8]. Although the Na⁺ ions in the interlayer of the parent NaLnTiO₄ occupied 9-coordinated site, the loaded protons in the interlayer of DLaTiO₄ occupied the sites different from the Na sites. That is, the loaded protons statistically occupied

Table 1
Structural parameters and final R values for $DLnTiO_4$ ($Ln = La, Nd$ and Y)

Sample	Atom	Site	g	x	y	z	U_{iso}^a (\AA^2)
$DLaTiO_4$ ^b	D	$16k$	1/8	0.114(1)	0.317(2)	0.4862(4)	0.037(1)
$P4/nmm$ (no. 129)	La	$2c$	1.0	0	1/2	0.8823(1)	0.0047(2)
$a = 3.7232(1) \text{\AA}$	Ti	$2c$	1.0	0	1/2	0.2991(2)	0.0093(7)
$c = 12.3088(1) \text{\AA}$	O1	$4f$	1.0	0	0	0.2563(1)	0.0064(3)
$R_{wp}^c = 2.69\%$	O2	$2c$	1.0	0	1/2	0.0772(2)	0.0077(4)
$R_p^d = 1.97\%$	O3	$2c$	1.0	0	1/2	0.4429(2)	0.0234(6)
$DNdTiO_4$	D	$16k$	1/8	0.069(4)	0.322(3)	0.4905(6)	0.061(4)
$P4/nmm$ (no. 129)	Nd	$2c$	1.0	0	1/2	0.8856(2)	0.0028(6)
$a = 3.7039(1) \text{\AA}$	Ti	$2c$	1.0	0	1/2	0.2923(4)	0.009(1)
$c = 12.0883(1) \text{\AA}$	O1	$4f$	1.0	0	0	0.2507(2)	0.0023(5)
$R_{wp} = 2.73\%$	O2	$2c$	1.0	0	1/2	0.0745(3)	0.006(1)
$R_p = 2.17\%$	O3	$2c$	1.0	0	1/2	0.4403(4)	0.021(1)
$DYTiO_4$	D1	$4e$	0.545(4)	0.464(4)	0.104(9)	0.319(10)	0.093(17)
$P2_1/c$ (no. 14)	D2	$4e$	0.454	0.537(3)	0.278(9)	0.133(6)	0.0061(19)
$a = 11.460(1) \text{\AA}$	Y	$4e$	1.0	0.8980(5)	0.023(2)	0.254(1)	0.003(2)
$b = 5.2920(4) \text{\AA}$	Ti	$4e$	1.0	0.2826(8)	-0.008(1)	0.246(3)	0.007(3)
$c = 5.3628(5) \text{\AA}$	O1	$4e$	1.0	0.230(2)	0.261(6)	0.007(4)	0.026(8)
$\beta = 90.441(9)^\circ$	O2	$4e$	1.0	0.768(2)	0.267(5)	0.006(4)	0.012(5)
$R_{wp} = 5.65\%$	O3	$4e$	1.0	0.063(1)	0.045(3)	0.222(2)	0.027(4)
$R_p = 4.14\%$	O4	$4e$	1.0	0.4298(9)	-0.010(3)	0.305(3)	0.013(4)

^a $B_{iso} = 8\pi^2 U_{iso}$.

^bRef. [6].

^c $R_{wp} = [\sum w_i(y_{io} - y_{ic})^2 / \sum w_i(y_{io})^2]^{1/2}$.

^d $R_p = \sum |y_{io} - y_{ic}| / \sum y_{io}$.

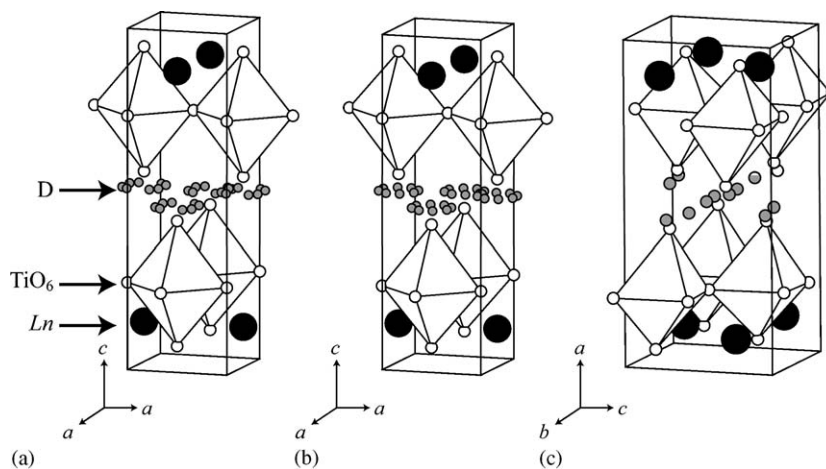


Fig. 3. Schematic illustrations of the crystal structures of (a) $DLaTiO_4$, (b) $DNdTiO_4$ and (c) $DYTiO_4$. It is noted that site occupancy factors of D atom in $DLnTiO_4$ ($Ln = La$ and Nd) and $DYTiO_4$ are 1/8 and 1/2 (mean value), respectively.

the sites around an apical O atom of a TiO_6 octahedron. Fig. 4 shows illustrations of local circumstance of the loaded protons bonding to the apical O atom of a TiO_6 octahedron in the interlayer. The D–O bond lengths were estimated to be 0.962(4) Å for $DLaTiO_4$, 0.930(7) Å for $DNdTiO_4$ and 0.72(4) and 1.22(4) Å for $DYTiO_4$. The D–O bond lengths for $DLaTiO_4$ and $DNdTiO_4$ and the mean D–O bond lengths of 0.97 Å for $DYTiO_4$ were close to the covalent O–H bond length, e.g., the O–H bond length in ethanol is 0.971 Å [15].

Fig. 5 shows the lattice parameters as a function of ionic radius of the rare-earth ion for $DLnTiO_4$ ($Ln = La, Nd$ and Y), together with those of the compound $NaLnTiO_4$ ($Ln = La, Pr, Nd, Sm, Eu, Gd, Y$ and Lu). The cell parameters of the orthorhombic and monoclinic systems were normalized to those of the tetragonal system, i.e., average of the $b/2^{1/2} + c/2^{1/2}$ lattice parameters and the a lattice parameter of orthorhombic and monoclinic systems were plotted as the a and c lattice parameters of the tetragonal system in Fig. 5, respectively. Whereas the a

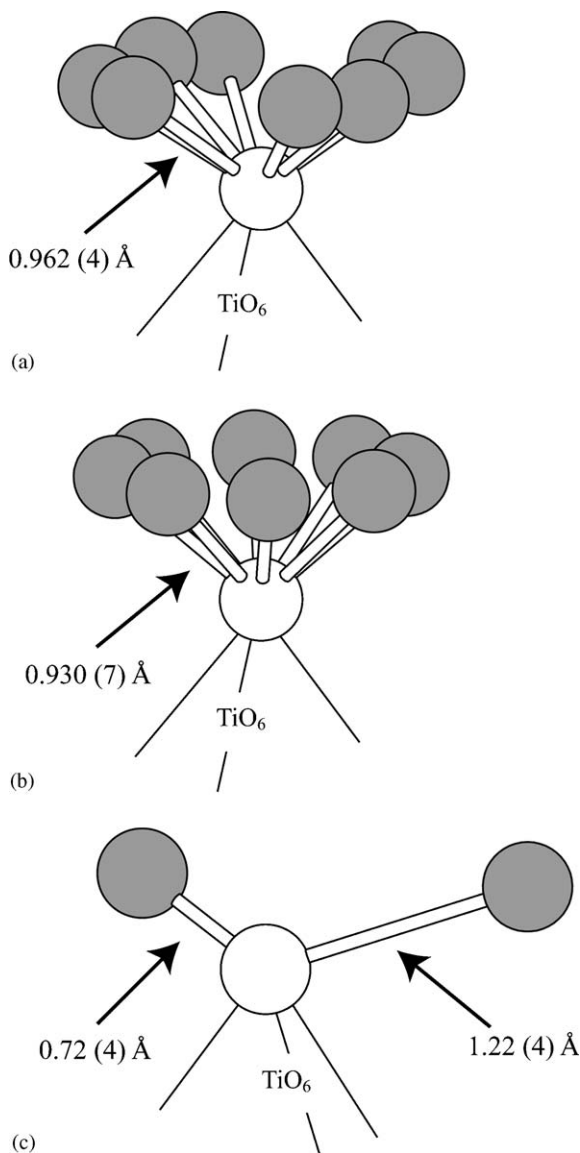


Fig. 4. Schematic illustrations of local circumstance of loaded proton bonding to the apical O atom of a TiO_6 octahedron in the interlayer of (a) DLaTiO_4 , (b) DNdTiO_4 and (c) DYTiO_4 . Gray circle, D; Open circle, O. It is noted that site occupancy factors of D atom in DLnTiO_4 ($\text{Ln} = \text{La}$ and Nd) and DYTiO_4 are 1/8 and 1/2 (mean value), respectively.

lattice parameters of NaLnTiO_4 were independent of the ionic radius of Ln^{3+} ion, the c lattice parameters were dependent on it. Furthermore, plots of the c lattice parameters for NaLnTiO_4 ($\text{Ln} = \text{rare earth}$) were bent at $\text{Ln} = \text{Nd}$. As mentioned above, the crystal structure of the parent compound changes from $P4/nmm$ ($\text{Ln} = \text{La-Nd}$) to $Pbcm$ ($\text{Ln} = \text{Sm-Lu}$ and Y) with decreasing ionic radius of Ln^{3+} ion. This structural change may lead the variety of the c lattice parameters to the bend in a series of NaLnTiO_4 ($\text{Ln} = \text{rare earth}$). The dependence of both the a and c lattice parameters of DLnTiO_4 ($\text{Ln} = \text{La, Nd}$ and Y) on the ionic radius of Ln^{3+} ion showed behaviors similar to those of NaLnTiO_4 ($\text{Ln} = \text{rare earth}$). The indexing of the XRD data of HGdTiO_4 , which was synthesized by the ion-exchange reaction from NaGdTiO_4 , was carried out on the

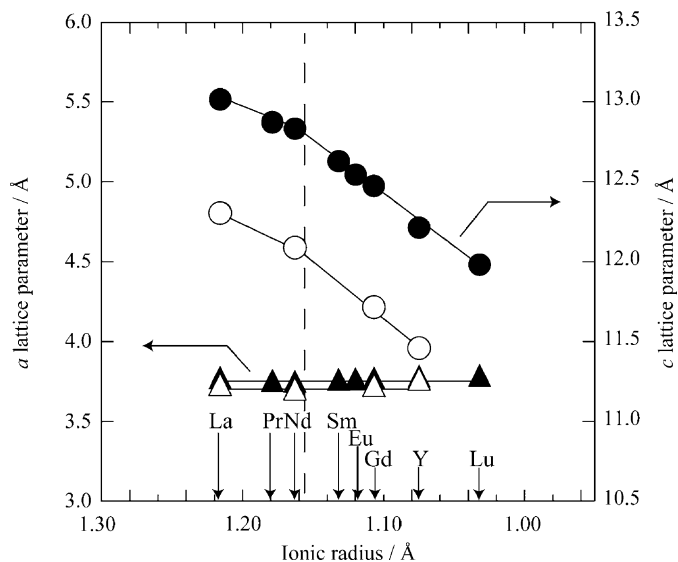


Fig. 5. The lattice parameters of DLnTiO_4 as a function of ionic radius of the rare-earth (Ln) ion. The cell parameters of the orthorhombic and monoclinic systems were normalized to those of the tetragonal system, i.e., average of the $b/2^{1/2} + c/2^{1/2}$ lattice parameters and the a lattice parameter of orthorhombic and monoclinic systems are plotted as the a and c lattice parameters of the tetragonal system, respectively. Open and filled symbols represent DLnTiO_4 and parent NaLnTiO_4 (Ref. [9]), respectively.

basis of the monoclinic system to confirm these behaviors. As a result, the estimated lattice parameters were successfully on the variety of the lattice parameters. Thus, the plots suggest that HGdTiO_4 crystallized in the monoclinic system with the same space group $P2_1/c$ as that of DYTiO_4 . It was, however, difficult to judge whether the HGdTiO_4 crystallized in the tetragonal system with the space group $P4/nmm$ or the monoclinic system with the space group $P2_1/c$, because neutron diffraction measurement cannot be performed due to the large absorption cross-section of gadolinium in HGdTiO_4 . Although the previous analyzed by the XRD reported that HLnTiO_4 ($\text{Ln} = \text{La, Nd, Sm}$ and Gd) crystallized in the tetragonal system with the space group $P4/nmm$ [9], the present exhibits that the crystal structures of HLaTiO_4 and HNdTiO_4 are different from those of HYTiO_4 (and HGdTiO_4). Consequently, it was considered that the crystal structure of HLnTiO_4 series changes between $\text{Ln} = \text{Nd}$ and Sm from $P4/nmm$ to $P2_1/c$, when the ionic radius of Ln^{3+} ion decreases.

4. Conclusions

Neutron diffraction study has concluded the crystal structure of DLnTiO_4 (HLnTiO_4 , $\text{Ln} = \text{La, Nd}$ and Y) prepared by the ion-exchange reaction of parent NaLnTiO_4 as follows: DLaTiO_4 and DNdTiO_4 crystallized in the tetragonal system with the space group $P4/nmm$, while DYTiO_4 crystallized in the monoclinic system with the space group $P2_1/c$. The loaded protons in the interlayer were statistically located at the sites different from the Na atom sites in the parent NaLnTiO_4 , i.e., the sites around

the apical O atom of the TiO_6 octahedron, and covalently bonded to the apical O atom. Furthermore, the cell parameters of DLnTiO_4 (HLnTiO_4 , $\text{Ln} = \text{La, Nd, Gd}$ and Y) as a function of the ionic radius of Ln^{3+} ion corresponded to the fact that the crystal structure of DLnTiO_4 ($\text{Ln} = \text{rare earth}$) series changes at between $\text{Ln} = \text{Nd}$ and Sm from the space group $P4/nmm$ to $P2_1/c$.

Acknowledgments

We thank Dr. F. Izumi of National Institute for Materials Science in Japan for kindly supplying RIE-TAN-TN program. This work was partly supported by The Okayama University 21st Century COE Program “Strategic Solid Waste Management of sustainable Society”.

References

- [1] G. Mangamma, V. Bhat, J. Gopalakrishnan, S.V. Bhat, *Solid State Ionics* 58 (1992) 303–309.
- [2] A.J. Jacobson, J.W. Johnson, J.T. Lewandowski, *Mater. Res. Bull.* 22 (1987) 45–51.
- [3] J. Gopalakrishnan, V. Bhat, *Mater. Res. Bull.* 22 (1987) 413–417.
- [4] M.M.J. Treacy, S.B. Rice, A.J. Jacobson, J.T. Lewandowski, *Chem. Mater.* 2 (1990) 279–286.
- [5] S. Uma, A.R. Raju, J. Gopalakrishnan, *J. Mater. Chem.* 3 (1993) 709–713.
- [6] S. Nishimoto, M. Matsuda, S. Harjo, A. Hoshikawa, T. Kamiyama, T. Ishigaki, M. Miyake, *J. Eur. Ceram. Soc.* 26 (2006) 725–729.
- [7] S.N. Ruddlesden, P. Popper, *Acta Crystallogr.* 10 (1957) 538–539.
- [8] K. Toda, Y. Kameo, S. Kurita, M. Sato, *J. Alloys Compd.* 34 (1996) 19–25.
- [9] S.H. Byeon, J.J. Yoon, S.O. Lee, *J. Solid State Chem.* 127 (1996) 119–122.
- [10] S.H. Byeon, S.O. Lee, H. Kim, *J. Solid State Chem.* 130 (1997) 110–116.
- [11] W.J. Zhu, H.H. Feng, P.H. Hor, *Mater. Res. Bull.* 31 (1996) 107–111.
- [12] S. Nishimoto, M. Matsuda, M. Miyake, *J. Solid State Chem.* 178 (2005) 811–818.
- [13] T. Ohta, F. Izumi, K. Oikawa, T. Kamiyama, *Physica B* 234–236 (1997) 1093–1095.
- [14] F. Izumi, T. Ikeda, *Mater. Sci. Forum* 321–324 (2000) 198–203.
- [15] M. Ohki (Ed.), *Handbook of Chemistry Basic*, fourth ed., Maruzen, Tokyo, 1993, p. II-656.